Original article

Pregnenolone 16α-carbonitrile negatively regulates hippocampal cytochrome P450 enzymes and ameliorates phenytoin-induced hippocampal neurotoxicity

Shuai Zhang [a, c], Tingting Wang [a, c], Ye Feng [d], Fei Li [e], Aijuan Qu [f, g], Xiuchen Guan [h], Hui Wang [b, c, **], Dan Xu [a, c, *]

[a] Department of Obstetric, Zhongnan Hospital of Wuhan University, School of Pharmaceutical Sciences, Wuhan University, Wuhan, 430071, China
[b] Department of Pharmacology, School of Basic Medical Sciences, Wuhan University, Wuhan, 430071, China
[c] Hubei Provincial Key Laboratory of Developmentally Originated Disease, Wuhan University, Wuhan, 430071, China
[d] Department of Endocrinology and Metabolic Disease, The First Affiliated Hospital, Zhejiang University School of Medicine, Hangzhou, 310058, China
[e] Frontiers Science Center for Disease-related Molecular Network, West China Hospital, Sichuan University, Chengdu, 610041, China
[f] Department of Physiology and Pathophysiology, School of Basic Medical Sciences, Capital Medical University, Beijing, 100069, China
[g] Key Laboratory of Remodeling-related Cardiovascular Diseases, Ministry of Education, Beijing, 100069, China
[h] Department of Orthodontics, School of Stomatology, Capital Medical University, Beijing, 100069, China

ARTICLE INFO

ABSTRACT

The central nervous system is susceptible to the modulation of various neurophysiological processes by the cytochrome P450 enzyme (CYP), which plays a crucial role in the metabolism of neurosteroids. The antiepileptic drug phenytoin (PHT) has been observed to induce neuronal side effects in patients, which could be attributed to its induction of CYP expression and testosterone (TES) metabolism in the hippocampus. While pregnane X receptor (PXR) is widely known for its regulatory function of CYPs in the liver, we have discovered that the treatment of mice with pregnenolone 16α-carbonitrile (PCN), a PXR agonist, has differential effects on CYP expression in the liver and hippocampus. Specifically, the PCN treatment resulted in the induction of cytochrome P450, family 3, subfamily a, polypeptide 11 (CYP3A11), and CYP2B10 expression in the liver, while suppressing their expression in the hippocampus. Functionally, the PCN treatment protected mice from PHT-induced hippocampal nerve injury, which was accompanied by the inhibition of TES metabolism in the hippocampus. Mechanistically, we found that the inhibition of hippocampal CYP expression and attenuation of PHT-induced neurotoxicity by PCN were glucocorticoid receptor dependent, rather than PXR independent, as demonstrated by genetic and pharmacological models. In conclusion, our study provides evidence that PCN can negatively regulate hippocampal CYP expression and attenuate PHT-induced hippocampal neurotoxicity independently of PXR. Our findings suggest that glucocorticoids may be a potential therapeutic strategy for managing the neuronal side effects of PHT.

1. Introduction

Cytochrome P450 enzyme (CYP) is a member of the heme-containing monooxygenases family that is responsible for catalyzing oxidation reactions and plays a crucial role in the metabolism of both endogenous and exogenous substances [1]. Although most CYPs are expressed and functional in the liver and intestine, they also have abundant expression in the central nervous system. Specifically, CYP isoforms in different brain regions are involved in the metabolism of neurosteroids and various exogenous substances, including psychoactive drugs [2].

The mammalian hippocampus is a crucial brain region that is responsible for learning, memory, and emotion regulation. Among the CYP isoforms that are expressed in the hippocampus, cytochrome P450, family 3, subfamily a (CYP3A), CYP2B, and CYP2C

have been identified [3,4]. The imbalance of CYPs in the brain has been linked to the neurotoxic side effects of certain drugs. For instance, the antiepileptic drug phenytoin (PHT) induces CYPs in the hippocampus, leading to increased CYP-mediated testosterone (TES) metabolism, which negatively impacts hippocampal neurogenesis and neuronal survival [5–10]. These effects may account for the clinical side effects of depression and cognitive impairment associated with this drug. Clinical and pre-clinical studies have demonstrated the neuroprotective effects of TES [11,12].

Drug or xenobiotic induction of CYP enzymes is often mediated by the so-called xenobiotic sensing nuclear receptors, such as pregnane X receptor (PXR), constitutive androstane receptor (CAR), and glucocorticoid receptor (GR). PXR, CAR, and GR are well known for their expression and regulation of CYPs in the liver and intestine. Among examples, PHT has been reported to induce the human CYP2B6 [13] and the mouse CYP2C29 [14] in a CAR dependent manner. PHT induces nuclear translocation and activation of CAR, and the activated CAR binds to the phenobarbital-responsive enhancer module/xenobiotic responsive enhancer module of CYP2B6 to promote the transcription [13]. Although these nuclear receptors that regulate CYPs are expressed in the central nervous system [15], their roles in the regulation of central CYPs are yet to be fully understood. Specifically, while PXR is a key regulator of CYPs in the liver, it has not been reported how the central PXR or its ligands may play a role in the regulation of CYPs and the metabolism of TES, and whether this regulation is involved in the neuronal side effects of PHT.

In this study, we found that the prototypical PXR agonist pregnenolone 16α-carbonitrile (PCN) attenuated PHT-induced hippocampal neurotoxicity by tissue-specifically suppressing the expression of CYPs in the hippocampus. The neuroprotective effect of PCN was independent of PXR, but instead may have been mediated by the glucocorticoid (GC)-GR signaling pathway.

2. Materials and methods

2.1. Animal and drug treatment

Male C57BL/6J mice aged 6–8 weeks and weighing 20 ± 2 g, were procured from the Animal Center of Hubei Province, China (Permit No.: SCXK 2015-0018) with specific pathogen free conditions. The experiments were conducted at the Animal Experimental Center of Wuhan University (Permit No.: 14016), which is accredited by the Association for Assessment and Accreditation of Laboratory Animal Care International for Laboratory Animal Evaluation and Care. The animal protocol adhered to the guidelines and principles of the Chinese Council on Animal Welfare for the Use and Care of Laboratory Animals. The animal holding environment was maintained with optimal conditions of temperature (18–22 °C), humidity (40–60%), excellent air ventilation, and a 12 h dark/12 h light circadian rhythm. Additionally, 6–8 weeks old male PXR knockout (KO) mice with a C57BL/6J background and weighing 20 ± 2 g were utilized, and the creation of these PXR KO mice was previously reported [16].

The animals were acclimated for one week before being treated with drugs through intraperitoneal injections. The drugs and their respective doses used in the study were as follows: 1) PHT (Sigma-Aldrich, St. Louis, MO, USA) at a dose of 20 mg/kg for 28 consecutive days, based on the established dose range of 12–75 mg/kg required for antiepileptic efficacy or neurological toxic side effects in rodents, and a minimum of 21 days of continuous administration [17–19]; 2) PCN (APExBIO, Houston, TX, USA) at a dose of 15 mg/kg administered every 3 days for a total of 9 doses over 28 days, considering the role of the blood-brain barrier in the central nervous system and the requirement of doses greater than 10 mg/kg to

exert central nervous system effects [20,21]; 3) dexamethasone (DEX, Sigma-Aldrich) at a dose of 4 mg administered every 3 days simultaneously with PCN for a total of 9 doses over 28 days, based on findings from previous studies reporting the inhibition of epileptiform activity in rats at a dose of 3 mg/kg DEX, and the potential for nerve damage at a dose of 5 mg/kg DEX administered to mice for 28 consecutive days [22,23]; and 4) mifepristone (RU486, APExBIO) at a dose of 10 mg/kg, selected based on previous reports of anti-glucocorticoid activity at doses greater than 5 mg/kg and the ability to cross the blood-brain barrier when administered at doses greater than 10 mg/kg [24].

2.2. Neuroethology

Male mice were utilized in this study to avoid the potential confounding factor of estrous cycle and were housed in the testing room for a week before ethology testing. The testing times were set from 8:00 a.m. to 6:00 p.m.

2.2.1. Elevated plus maze

The apparatus utilized in the experiment consisted of two open and closed arms connected by a central platform area. Prior to the start of the experiment, the apparatus was cleaned using 75% ethanol to prevent any odors or effects of animal secretions on the test results. At the beginning of the experiment, the mice were placed in the central platform area and allowed to move freely for a duration of 5 min. The recorded data was analyzed using the SMART 3.0 system (Panlab, Holliston, MA, USA).

2.2.2. Open field test

The open field apparatus utilized in this study was a blackened open box. The mice were placed in the center of the area, and their activity was recorded for a duration of 5 min using a video camera. The open field was divided into 25 grids via computer software, and the activity of the mice as well as any depression-like behavior were assessed by analyzing their movements on the grid.

2.2.3. Morris water maze

The experimental apparatus consisted of medially darkened round cylinders, which were artificially divided into four quadrants, with the platform placed in one of the quadrants, not submerged by 2–4 cm. The experiment was divided into two phases: the training test and the exploration test. During the training test phase, the mice were sequentially placed into the water from the four different quadrants, facing the round cylinders, at a water temperature of 22 ± 1 °C. The camera recorded the movement of the mice in the water during a 90 s period. If the mice were unable to find the platform within 60 s, they were guided to the upper platform. Following four consecutive training sessions, on the fifth day, the mice were placed in the water from a certain quadrant, and the time spent on the upper platform was recorded. During the exploration test phase, the platform was withdrawn, and the movements of the mice were observed for a period of 60 s.

2.3. Real-time quantitative reverse transcription-polymerase chain reaction (RT-qPCR)

Total RNA was isolated using QIAzol Lysis Reagent (Qiagen, Hilden, Germany), with genomic DNA contamination eliminated using TURBO-DNase (Ambion, Austin, TX, USA). Reverse transcription of RNA was performed using the iScriptTM cDNA Synthesis Kit (Bio-Rad, Hercules, CA, USA). The relative quantification of gene expression was determined using the ΔΔCq method on the Applied Biosystems 7300 real-time PCR system (Applied Biosystems, Bedford, MA, USA) with iTaq SYBR Green Supermix and

ROX (Bio-Rad). The expression of the house-keeping gene glyceraldehyde 3-phosphate dehydrogenase (*Gapdh*) was used for normalization of the PCR results. The primer sequences utilized in the study are listed in Table S1.

2.4. Western blotting

Following euthanasia, the hippocampus was rapidly dissected on ice, snap-frozen, and stored at −80 °C until analysis. The frozen brain samples were allowed to thaw on ice and then homogenized in 5 volume of ice-cold homogenization buffer (phosphate buffer saline (PBS; PWL101, Meilunbio, Dalian, China) containing 0.2% NP-40 and protease inhibitor). Homogenates were centrifuged at 15,000 *g* for 20 min at 4 °C, and the supernatants were utilized to measure protein concentrations using the bicinchoninic acid method. A total of 25 μg of each sample was further diluted in sample buffer (Bio-Rad), and sodium dodecyl sulfate-polyacrylamide gel electrophoresis (SDS-PAGE) was performed using 15% polyacrylamide gels. The proteins were then transferred to polyvinylidene fluoride membranes and probed with primary antibodies against cytochrome P450, family 3, subfamily a, polypeptide 11 (CYP3A11) (dilution of 1:500, kindly provided by Dr. Frank J. Gonzalez, National Institutes of Health (NIH), USA), mouse CYP2B10 (dilution of 1:1,500, Sigma-Aldrich), β-actin (dilution of 1:1,000, Santa Cruz Biotechnology, Santa Cruz, CA, USA), or GAPDH (dilution of 1:2,000, Abclonal, Wuhan, China), followed by incubation with horseradish peroxidase-conjugated secondary antibodies (dilution of 1:20,000, BD Diagnostic Systems, Sparks, MD, USA). Immunoreactive proteins were visualized using an enhanced chemiluminescence detection system (Thermo Fisher Scientific Inc., Waltham, MA, USA). Semi-quantification of individual bands was performed using ImageJ software (NIH-Image 1.42q, Bethesda, MD, USA) by plotting density. The relative expression of target proteins was normalized against β-actin or GAPDH.

2.5. Nissl staining

The brain tissues were fixed with 4% paraformaldehyde at 4 °C for 18 h, embedded using optimum cutting temperature compound at −80 °C, and sectioned at 35 μm using a sliding microtome (CM1950, Leica Microsystems GmbH, Wetzlar, Germany). Following washing with PBS at pH 7.4, the tissues were dried at 55 °C for 3 h and immersed in 0.9% crystal violet at 37 °C (Sigma-Aldrich) for 2 h. The tissues were then sequentially dehydrated with 70%, 80%, 90%, and 100% ethanol for 5 min and mounted with neutral balsam. The sections were visualized using a fluorescent microscope (100 μm, Eclipse 80i, Nikon Corporation, Tokyo, Japan). Densitometric analysis and determination of the mean analysis area of Nissl body positive cells were performed using ImageJ software.

2.6. Golgi staining

The Golgi staining technique was utilized to investigate the morphology of neurons in the hippocampus. The study employed a rapid Golgi staining kit (FD NeuroTechnologies, Ellicott City, MD, USA) following the manufacturer's protocol. The analysis involved the quantification of spines along the first 15−30 μm of the first primary dendrite emanating from the large apical dendrites. The study included only cells with well-defined dendrites and easily identifiable secondary structures and soma, and cells were randomly selected within the selected fields. To determine relative spine density, the total numbers were normalized to reflect per 10 μm number of spanning dendrites. The primary dendrite length and secondary branching were evaluated through sholl analysis.

Five neurons per section were captured using Nikon act-1 software, totaling 3 per animal section and analyzed in ImageJ by a blind observer. The total length of dendritic and branching intersections represents the sum of sholl outputs up to 150 μm away from the soma. The total number of primary branches was also calculated from the same area of the hippocampus for comparison and data analysis.

2.7. Immunohistochemistry (IHC)

IHC was carried out to investigate the expression of various proteins in mouse brains. The brains were dissected and fixed overnight in Hartman's fixative (Sigma-Aldrich), embedded in optimal cutting temperature compound at −80 °C, and sectioned at 15 μm. The tissue sections were blocked with 10% bovine serum albumin at 4 °C overnight and incubated with primary antibodies specific to CYP3A11 (1: 200 dilution, kindly provided by Dr. Frank J. Gonzalez, NIH, USA), CYP2B10 (1:300 dilution, Sigma-Aldrich), PXR (1:100 dilution, ab217375, Abcam, Cambridge, MA, USA), or GR (1:150 dilution, ab3578, Abcam). The slides were then incubated with a biotinylated secondary antibody (1:3,000 dilution, BA9500, Vector Laboratories, Newark, CA, USA) for 3 h at room temperature. Subsequently, each slide was immersed in color reagent avidin-biotin complex (1:200 dilution, ABC staining system, PK-6100, Vector Laboratories) diluted in PBS for 3 min in the dark and then mounted with neutral balsam. The semi-quantitative analysis of IHC was performed using the ImageJ plugin IHC-Toolbox [25]. The color deconvolution function of IHC-Toolbox was utilized to mark and distinguish the cells with positive expression of PXR, CYP3A11, CYP2B10, or GR protein, and the gray value was used to calculate the degree of positive expression. To calculate the percentage of positive expressing cells in total cells, we used the IHC-Toolbox and IHC Profiler plugin. Cells with an area of positive expression greater than 65% were classified as positive cells, while those with an area of positive expression less than 65% were classified as negative cells. Please refer to Fig. S1 for the specific principle and process.

2.8. Liquid chromatography-tandem mass spectrometry (LC-MS/MS)

The quantification of TES and 6beta-hydroxytestosterone (6β-OH-TES) in brain tissues and serum was conducted using LC-MS/MS. Brain tissues were homogenized and extracted with diethyl ether, as previously described [26], before being subjected to LC-MS/MS analysis. The LC-MS/MS system utilized a two-dimensional chromatography system and an AB/Sciex QTrap 5500 tandem mass spectrometer (SCIEX, Framingham, MA, USA) in atmospheric pressure chemical ionization positive and electrospray ionization negative ion mode, respectively. Total TES and 6β-OH-TES were quantified in the brain tissue extracts or serum using LC-MS/MS without derivatization. To investigate the kinetics of testosterone metabolism, we employed the ultracentrifugation method instead of the calcium chloride aggregation method to extract brain tissue microsomes in order to preserve the activity of CYP enzymes as previously reported [27]. The incubation mixture (200 μL) consisted of Tris-HCl buffer (150 mM KCl, 50 mM Tris, and 10 mM $MgCl_2$, pH 7.4), 1.25 mM nicotinamide adenine dinucleotide phosphate (NADPH), 0.5 mg protein/mL microsomes, and testosterone (at final concentrations of 25, 50, 75, 100, 125, 150, 175, 200, 225, 250, 275, 300, 325, 350, and 375 μM). The reaction was initiated by the addition of NADPH at 37 °C and terminated by the addition of cold acetonitrile.
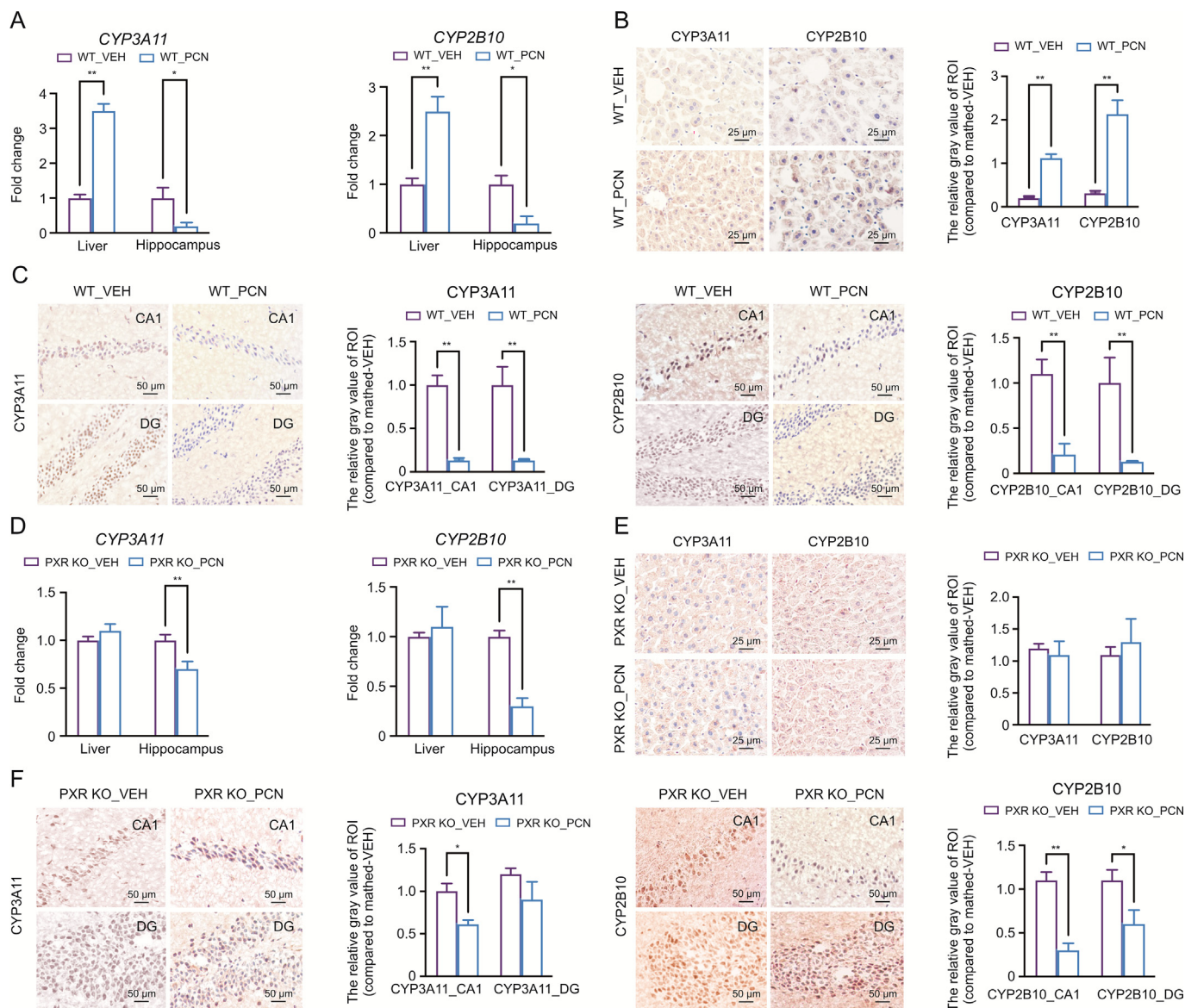
Fig. 1. Pregnenolone 16α-carbonitrile (PCN) suppresses the hippocampal cytochrome P450 enzyme expression independent of pregnane X receptor (PXR). (A–C) Wild-type (WT) male mice were treated with vehicle (VEH) or PCN for four weeks before tissue harvesting (*n* = 6). The messenger RNA (mRNA) expressions measured by real-time quantitative reverse transcription-polymerase chain reaction (RT-qPCR) of cytochrome P450, family 3, subfamily a, polypeptide 11 (*CYP3A11*), and *CYP2B10* in the liver and hippocampus (A) and immunohistochemistry (IHC) staining for CYP3A11 and CYP2B10 in the liver (B) and the hippocampus (C). (D–F) PXR knockout (PXR KO) mice were treated with VEH or PCN for four weeks before tissue harvesting (*n* = 6). The mRNA expressions measured by RT-qPCR of *CYP3A11* and *CYP2B10* in the liver and hippocampus (D) and IHC staining for CYP3A11 and CYP2B10 in the liver (E) and in the hippocampus (F). The IHC results were semi-quantified by ImageJ scripts of IHC-Toolbox. Data are presented as mean ± standard error of the mean. $^{*}P < 0.05$ and $^{**}P < 0.01$. ROI: region of interest; CA1: cornu ammonis area 1; DG: dentate gyrus.

2.9. Bioinformatic analysis of Gene Expression Omnibus (GEO) microarray data

The dataset GSE2880 form GEO was subjected to bioinformatic analysis. Hippocampal tissue treated with PHT and its corresponding vehicle control group were extracted for further analysis. The differential gene expression analysis was performed using the R package limma. The target-genes that were activated or inactivated by GR were obtained through a literature search and were utilized by the EnhancedVolcano package to generate volcano plots. Differential genes with an absolute log-fold change (|logFC|) greater than 0.5 and a *P* value less than 0.05 were selected for enrichment pathway analysis using the ClusterProfiler R package. The code

used for the analysis is accessible at Github (https://github.com/zhsh006/PXR_Pub).

2.10. Statistical analysis

Statistical analyses were conducted using GraphPad Prism v9.1.1 (GraphPad Software, San Diego, CA, USA). Differences between two groups or more were analyzed using Student *t*-test and one-way analysis of variance (ANOVA) followed by Bonferroni's post-hoc test, respectively. Two-way ANOVA was performed when the analysis included two independent variables. The evolution of groups over time was assessed using repeated measures ANOVA. All statistical tests were two-tailed, and *P* values less than 0.05 were
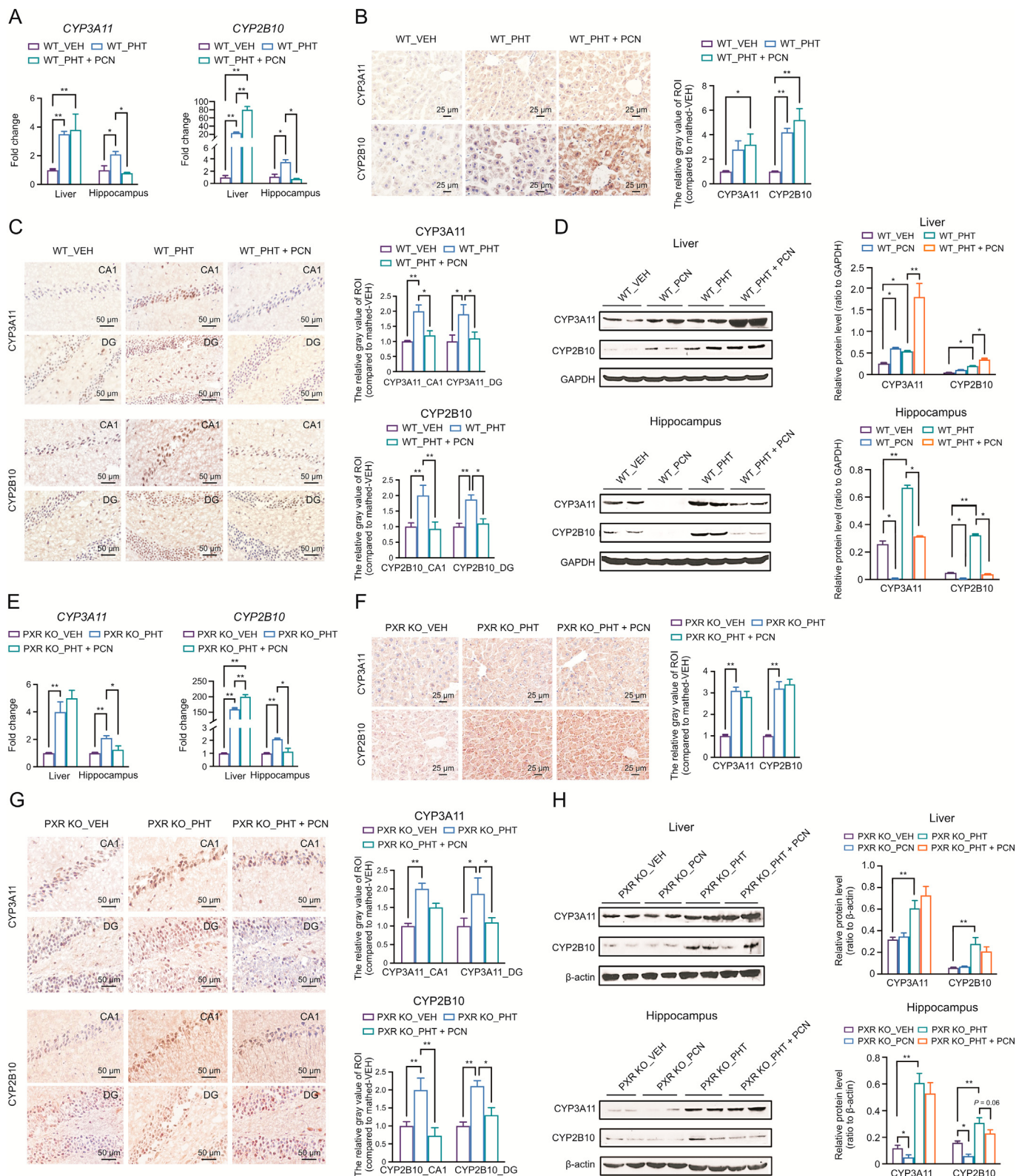
Fig. 2. Pregnenolone 16α-carbonitrile (PCN) reverses phenytoin (PHT)-responsive induction of cytochrome P450 enzyme in the hippocampus independent of pregnane X receptor (PXR). (A−D) Male wild-type (WT) mice were treated with vehicle (VEH), PHT, PCN, or PHT + PCN for four weeks before tissue harvesting ($n = 6$). The messenger RNA (mRNA) expressions measured by real-time quantitative reverse transcription-polymerase chain reaction (RT-qPCR) of cytochrome P450, family 3, subfamily a, polypeptide 11 (*CYP3A11*), and *CYP2B10* in the liver and hippocampus (A), immunohistochemistry (IHC) staining for CYP3A11 and CYP2B10 in the liver (B) and the hippocampus (C), and Western blotting for CYP3A11 and CYP2B10 in the liver and hippocampus (D). (E−H) PXR knockout (PXR KO) mice were treated with VEH, PHT, PCN, or PHT + PCN for four weeks before tissue harvesting ($n = 6$). The mRNA expressions measured by RT-qPCR of *CYP3A11* and *CYP2B10* in the liver and hippocampus (E), IHC staining for CYP3A11 and CYP2B10 in the liver (F) and the hippocampus (G), and Western blotting for CYP3A11 and CYP2B10 in the liver and hippocampus (H). The IHC results were semi-quantified by ImageJ scripts of IHC-Toolbox. Data are presented as mean ± standard error of the mean. *$P < 0.05$, ROI: region of interest; **$P < 0.01$. CA1: cornu ammonis area 1; DG: dentate gyrus; GAPDH: glyceraldehyde 3-phosphate dehydrogenase.
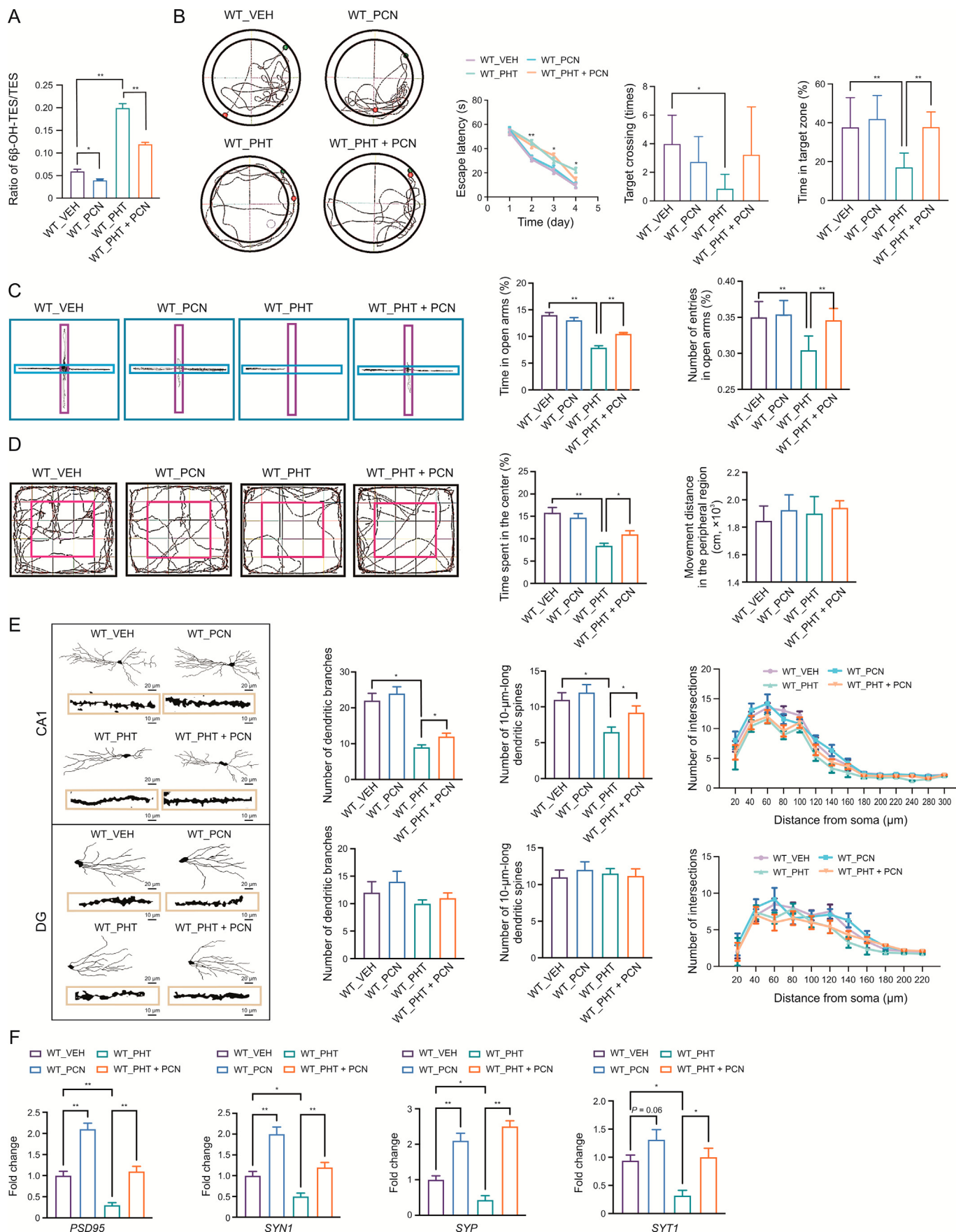
considered to be statistically significant. The data are presented as mean ± standard error of the mean.

3. Results

3.1. PCN suppresses the hippocampal CYP expression independent of PXR

In this study, we investigated the regulatory effect of hippocampal PXR on CYP expression by administering PCN, a potent agonist for mouse PXR, to mice and measuring the expression of CYPs in the hippocampus. As expected, PCN treatment increased the messenger RNA (mRNA) expression of *CYP3A11* and *CYP2B10* in the liver, as shown in Fig. 1A. Surprisingly, we observed a decrease in the mRNA expression of *CYP3A11* and *CYP2B10* in the hippocampus of the same PCN-treated mice, indicating that PCN had an opposite effect on CYP expression in the liver and hippocampus. This tissue-specific effect of PCN on CYP expression was further confirmed by immunohistochemical staining of CYP3A11 and CYP2B10 proteins in the liver (Figs. 1B and S2A) and in the cornu ammonis area 1 (CA1) and dentate gyrus (DG) regions of the hippocampus (Figs. 1C, S2B, and S2C). These findings suggest that PCN specifically suppresses CYP expression in the hippocampus.

To determine whether the suppression of hippocampal CYPs by PCN was dependent on PXR, we utilized PXR KO mice in our study. As expected, the mRNA expression of *CYP3A11* and *CYP2B10* in the liver was not induced upon PCN treatment in PXR KO mice, as shown in Fig. 1D. However, we observed that the mRNA expression of *CYP3A11* and *CYP2B10* in the hippocampus remained suppressed in PCN-treated PXR KO mice, indicating that PCN suppressed hippocampal CYP expression in a PXR-independent manner. This observation was further supported by immunohistochemical staining of CYP3A11 and CYP2B10 proteins in the liver (Figs. 1E, and S2D) and hippocampus (Figs. 1F, S2E, and S2F) of PXR KO mice, which showed the same pattern of PCN effect as in wild-type (WT) mice. These findings suggest that the suppression of hippocampal CYP expression by PCN is not dependent on PXR.

3.2. PCN reverses PHT-responsive induction of CYPs in the hippocampus independent of PXR

The administration of PHT, an antiepileptic drug, is known to cause depression and cognitive impairment in certain patients [6,28], which is attributed to the induction of hippocampal CYP3A and the consequent increase in TES metabolism [29,30]. Long-term PHT administration is also reported to cause CYP3A11 induction and CYP3A-dependent depletion of TES in CA1 pyramidal neurons [29]. In this study, we investigated whether PCN could attenuate the PHT-responsive induction of CYPs in the hippocampus. WT mice were treated with vehicle, PHT alone, or PHT together with PCN. The mRNA expression of *CYP3A11* and *CYP2B10* in the liver was induced by PHT as expected (Fig. 2A). Co-treatment with PCN showed little effect on the mRNA expression of *CYP3A11* but further increased the mRNA expression of *CYP2B10* (Fig. 2A). In the hippocampus, PHT alone induced the mRNA expression of CYP3A11

and CYP2B10, consistent with prior reports [29]. However, co-treatment with PCN attenuated the hippocampal induction of *CYP3A11* and *CYP2B1*0 by PHT (Fig. 2A). The pattern of effect of PHT and PHT + PCN on the protein level of CYP3A11 and CYP2B10 in the liver (Figs. 2B, 2D (left), and S2G) and hippocampus (Figs. 2B, 2D (right), S2H, and S2I) was confirmed by both IHC and Western blotting. These findings suggest that PCN may have therapeutic potential to mitigate the side effects of PHT on the hippocampus by attenuating the PHT-responsive induction of CYPs.
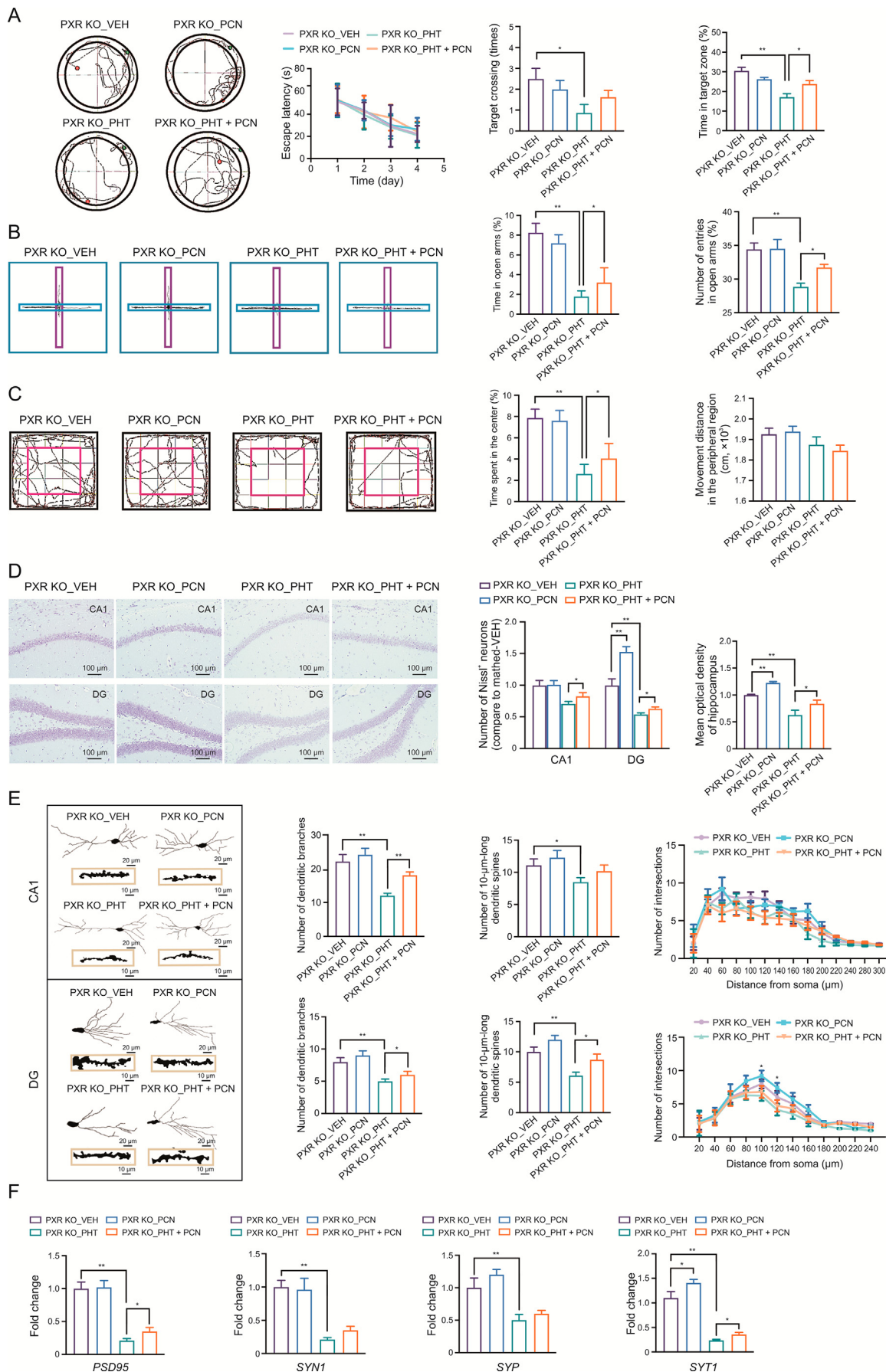
To investigate whether the attenuation of PHT-responsive hippocampal induction of CYPs by PCN was PXR-dependent, the drug treatments were repeated in PXR KO mice. The results showed that PHT treatment increased the mRNA expression of *CYP3A11* and *CYP2B10* in the liver of PXR KO mice (Fig. 2E), and there was no significant difference in the *CYP3A11* induction between PHT and PHT + PCN groups. However, the induction of *CYP2B10* was modestly but significantly further increased in the PHT + PCN group compared with the PHT group (Fig. 2E). The mechanism for the further induction of *CYP2B10* in the PHT + PCN group remains to be defined, but it is possible that chronic treatment with PCN in PXR KO mice may have induced *CYP2B10* by contributing to CAR activation. In the hippocampus, PHT increased the mRNA expression of *CYP3A11* and *CYP2B10* (Fig. 2E), but these increases were attenuated by the co-treatment of PCN (Fig. 2E). The pattern of effect of PHT and PHT + PCN on the protein expression of CYP3A11 and CYP2B10 in the liver (Figs. 2F, 2H (left), and S2J) and hippocampus (Figs. 2G, 2H (right), S2K, and S2L) was confirmed by both IHC and Western blotting. These results suggest that PCN can reverse the PHT-responsive induction of CYP in the hippocampus independent of PXR.

3.3. Treatment with PCN attenuates the neurotoxic side effects of PHT

Given that the neurotoxic side effects of PHT are attributed to the abnormal elevation of CYPs and subsequent increase in TES metabolism in the hippocampus, the authors sought to investigate whether PCN could reverse these effects by suppressing CYP expression and recovering TES activity. Specifically, the authors aimed to determine whether PCN could reverse the neurotoxic side effects of PHT by attenuating CYP induction and restoring TES levels in the hippocampus.

To establish a mouse model of neuronal side effects of PHT, 6-week-old male mice were treated with PHT for 4 weeks and evaluated for neurobehavioral changes using the Morris water maze test, elevated plus maze test, and open field experiment. The Morris water maze test revealed that PHT treatment impaired the learning and memory of mice, as evidenced by their elevated escape latency in the training phase and decreased residence time in the target quadrant and crossing times (Fig. S3A). The elevated plus maze test showed that the residence time of PHT-treated mice in the open arm was significantly lower than that of the vehicle group (Fig. S3B), indicating anxiety-like behavioral changes. The open field experiment demonstrated that PHT treatment reduced the exploratory activity of mice, as evidenced by their decreased time

Fig. 3. Treatment with pregnenolone 16α-carbonitrile (PCN) attenuates the neurotoxic side effects of phenytoin (PHT). Wild-type (WT) male mice were treated with vehicle (VEH), PCN, PHT, or PHT + PCN for four weeks before analyses (*n* = 8). (A) The ratio of 6β-hydroxytestosterone (6β-OH-TES) to testosterone (TES) in the hippocampus measured by liquid chromatography-tandem mass spectrometry. (B) Morris water maze results with the escape latency recorded, and the crossing number and residence time in the target quadrant calculated. (C) Elevated plus maze results with the elevated activity track, the stay time, and the entry number in the open arms calculated. (D) Open field test results with the residence time in the central area, and the movement distance in the peripheral region calculated. (E) The hippocampus sections were subjected to Golgi staining, and representative images of the neurite tracing profiles of neurons in the cornu ammonis area 1 (CA1) and dentate gyrus (DG) region. Statistics were performed separately for branch number, dendritic spine density, and dendritic branch nodes. (F) Hippocampal messenger RNA (mRNA) expressions of *PSD95*, *SYN1*, *SYP*, and *SYT1* were measured by real-time quantitative reverse transcription-polymerase chain reaction (RT-qPCR). Data are presented as mean ± standard error of the mean. *$^*P < 0.05$ and *$^{**}P < 0.01$.

spent in the central region, but increased their activity in the peripheral region (Fig. S3C). These findings suggest that PHT treatment induces neurobehavioral changes in mice, including impaired learning and memory, anxiety-like behavior, and altered exploratory activity.

To examine the histological effects of PHT-induced neurotoxicity, Nissl staining was performed on hippocampus tissue sections. The results showed that the Nissl body-positive neurons in the hippocampus CA1 and CA3 regions of PHT-treated mice were lower than those in the vehicle group (Fig. S3D). The Nissl body-positive neurons in the DG region also tended to be lower, although the difference did not reach statistical significance (Fig. S3D). The mean optical density analysis of the entire hippocampus indicated that the intensity of Nissl staining in PHT-treated mice was lower than that in the vehicle group. Furthermore, the hippocampal neurons in the CA3 region of PHT-treated mice exhibited signs of central Nissl body dissolution, with the disappearance of cytoplasmic central Nissl body and appearance of Nissl body remnants around it (Fig. S3E). The hippocampal neurons in PHT-treated mice also showed vacuolation, suggesting that PHT may have inhibited neuroprotein synthesis. Consistent with this, the mRNA expressions of *PSD95*, *SYN1*, *SYP*, and *SYT1* were decreased in PHT-treated mice (Fig. S3F). These findings suggest that PHT-induced neurotoxicity is associated with histological changes in the hippocampus, including reduced Nissl body-positive neurons, vacuolation, and inhibition of neuroprotein synthesis.

It has been established that CYP3As play a crucial role in the metabolism of TES to produce 6β-OH-TES, which is known to have limited hormonal activity, ultimately leading to TES deactivation [31]. To eliminate the influence of hepatic metabolism, we measured the levels of TES and 6β-OH-TES in the hippocampal tissue rather than TES level in the blood. Initially, we evaluated the activity of CYP enzymes in the liver and hippocampus, as shown in Fig. S4A, and observed that both liver and hippocampus microsomes exhibited high testosterone-metabolizing enzyme activity in vitro. Additionally, enzyme activity assays of hippocampal microsomes from each group indicated that PHT accelerated the metabolism of TES in the hippocampus, while PCN inhibited the metabolism of TES in the hippocampus, although the inhibitory effect was not particularly strong in vitro. In liver microsome assays, both the PCN group and PHT group increased the metabolism of testosterone (Fig. S4B). Furthermore, as shown in Fig. 3A, we observed an increase in the ratio of 6β-OH-TES to TES in the hippocampus of PHT-treated mice, consistent with the CYP induction in this region. This effect was also reversed by PCN treatment. These findings suggested that PHT treatment enhanced the metabolism of TES in the hippocampus, and this effect can be reversed by co-treatment with PCN.

The observed decrease in neurosteroid levels, including TES, has been implicated in the neuronal side effects associated with PHT treatment [29]. Our findings suggest that the induction of hippocampal CYPs and subsequent increased metabolic deactivation of TES may serve as a plausible mechanism underlying PHT-induced neurobehavioral and hippocampal neurotoxic side effects. Conversely, our results indicate that treatment with PCN alone decreased the ratio of 6β-OH-TES to TES and, when co-administered

with PHT, attenuated PHT-induced TES metabolism as depicted in Fig. 3A. These findings are consistent with the established pattern of CYP regulation by PCN in the hippocampus.

To ascertain whether the observed attenuation of PHT-induced TES metabolism by PCN translates to amelioration of PHT-induced neurobehavioral changes and hippocampal neurotoxicity, we conducted further experiments. Our results, as shown in Fig. 3B, demonstrate that the PHT-induced impairment of learning and memory, as evidenced by higher escape latency in the training stage, and lower crossing times and residence time in the target quadrant, was attenuated in the PHT + PCN group during the Morris water maze test. Similarly, in the elevated plus maze test, the PHT-induced decrease in stay time and entry time in the open arm were attenuated in the PHT + PCN group, as depicted in Fig. 3C. Furthermore, in the open field experiment, the decreased time-taken induced by PHT was attenuated in the PHT + PCN group (Fig. 3D), without affecting the total movement distance of the mice in the open field. Collectively, these findings suggest that PCN treatment effectively protects against PHT-induced neurobehavioral damage.

We subsequently conducted Golgi staining on the hippocampal sections to assess the effect of PHT and PCN on the dendritic branches and spines of hippocampal neurons. Our results, as illustrated in Fig. 3E (top panels), indicate that PHT treatment significantly reduced the number of dendritic branches and spines of hippocampal neurons in the CA1 region, an effect that was effectively attenuated by co-treatment with PCN. However, PHT treatment, in the absence or presence of PCN co-treatment, had little effect on the number of dendritic branches and spines of hippocampal neurons in the DG region, as depicted in Fig. 3E (bottom panels). Furthermore, among the hippocampal synaptic protein genes, we observed that PHT-responsive down-regulation of *PSD95*, *SYN1*, *SYP*, and *SYT1* was attenuated in the PHT + PCN group, as shown in Fig. 3F. These findings suggest that PCN treatment exerts a protective effect against PHT-induced hippocampal neuron injury, particularly in the CA1 region.

3.4. The neuroprotective effect of PCN is independent of PXR

Given that PCN has been shown to reverse PHT-responsive hippocampal induction of CYPs independent of PXR, we sought to investigate whether the neuroprotective effect of PCN is also PXR-independent. To this end, we evaluated the effect of PCN on PHT-induced neurobehavioral changes and nerve injury in PXR KO mice. Our results, as presented in Fig. 4A, indicate that PHT treatment effectively lowered the target quadrant in the Morris water maze behavior test, an effect that was attenuated by co-treatment with PCN. Similarly, in the elevated plus maze test, PHT treatment reduced the entries to the open arms and the time stay in the open arms of PXR KO mice, an effect that was also attenuated by PCN co-treatment, as depicted in Fig. 4B. Furthermore, in the open field experiment, PHT treatment lowered the residence time of PXR KO mice in the central area without affecting the total movement distance, an effect that was effectively attenuated by the co-treatment of PCN, as illustrated in Fig. 4C. These findings suggest that the neuroprotective effect of PCN is independent of PXR.

Fig. 4. The neuroprotective effect of pregnenolone 16α-carbonitrile (PCN) is independent of the pregnane X receptor (PXR). Male PXR knockout (PXR KO) mice were treated with vehicle (VEH), PCN, phenytoin (PHT), or PHT + PCN for four weeks before analyses (*n* = 6). (A) Results of Morris water maze with the escape latency recorded, and the crossing number and residence time in the target quadrant calculated. (B) Results of elevated plus maze with the elevated activity track, the stay time, and the entry number in the open arms calculated. (C) Results of open field test with the residence time in the central area and the movement distance in the peripheral region calculated. (D) Representative images of the Nissl staining with the number of Nissl body-positive neurons and the mean optical density of hippocampus calculated. (E) The hippocampus sections were subjected to Golgi staining, and representative images of the neurite tracing profiles of neurons in the cornu ammonis area 1 (CA1) and dentate gyrus (DG) region. Statistics were performed separately for branch number, dendritic spine density, and dendritic branch nodes. (F) Hippocampal messenger RNA (mRNA) expressions of *PSD95*, *SYN1*, *SYP*, and *SYT1* were measured by real-time quantitative reverse transcription-polymerase chain reaction (RT-qPCR). Data are presented as mean ± standard error of the mean. $^*P < 0.05$ and $^{**}P < 0.01$.
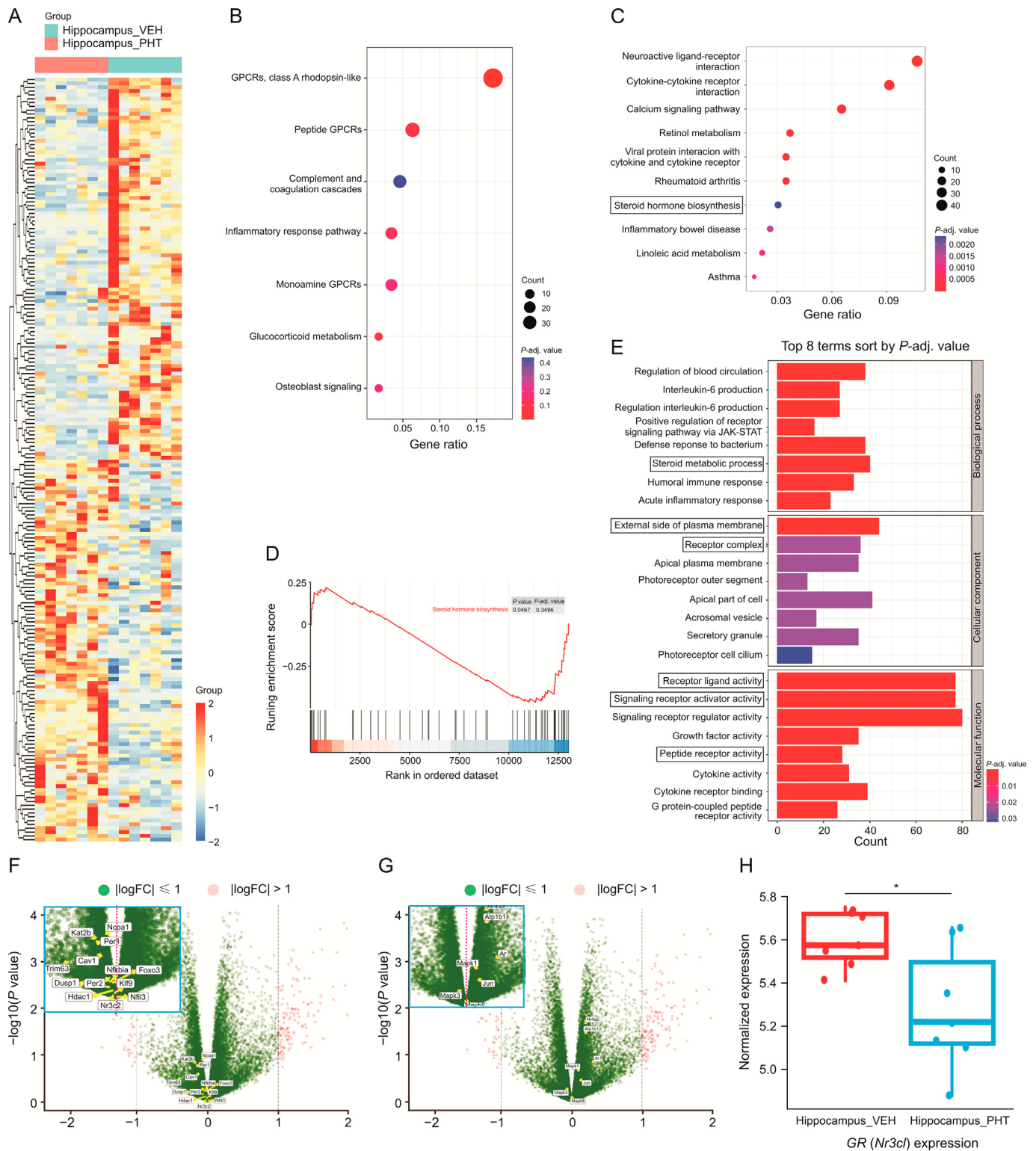
Fig. 5. Bioinformatic analysis reveals that phenytoin (PHT)-induced neurotoxicity is accompanied by suppression of glucocorticoids/glucocorticoid receptor (GR) signaling in the hippocampus. (A) Heatmap for the top 200 differentially expressed genes (DEGs) upon the PHT treatment. (B) DEGs enriched for Wiki Pathway analyzed using the R package ClusterProfiler. (C, D) Top 10 enriched Kyoto Encyclopaedia of Genes and Genomes (KEGG) pathways (C) and gene set enrichment analysis of the 'Steroid hormone biosynthesis' pathway (D). (E) DEGs enriched for Gene Ontology (GO) terms. 'Z-score' showed that most of steroid metabolic-related biological processes show an upward trend. (F, G) The Volcano map for DEGs with target-genes activated (F) or suppressed (G) by GR labelled. (H) The hippocampal messenger RNA (mRNA) expression of *GR* (*Nr3c1*) in the vehicle (VEH) and PHT groups. Red dots: genes with |logFC| > 1; blue dots: genes with |logFC| ≤ 1. *$P < 0.05$. GPCRs: G-protein-coupled receptors; JAK-STAT: Janus kinase-signal transducer and activator of transcription; FC: fold change.
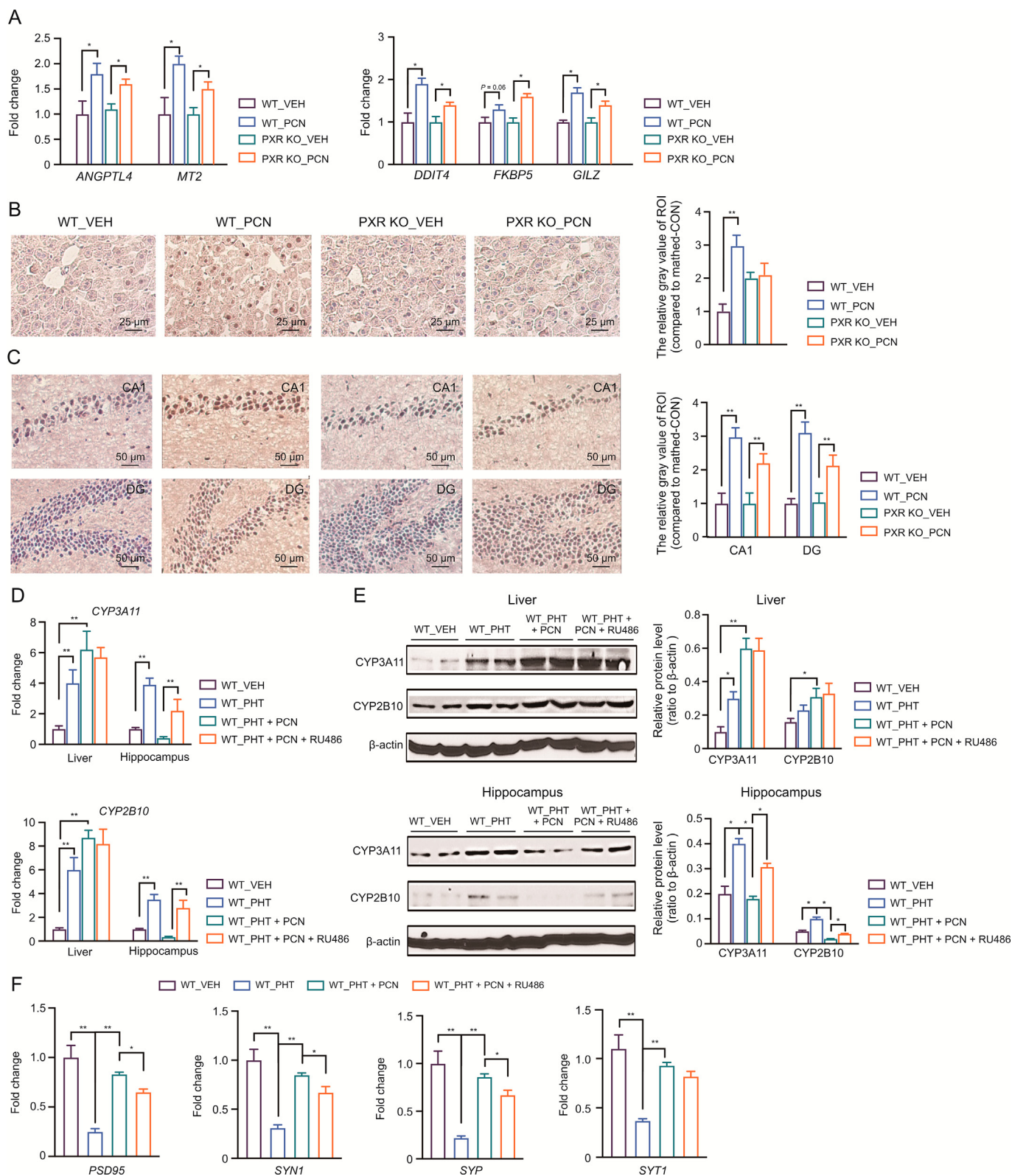
Fig. 6. Treatment with pregnenolone 16α-carbonitrile (PCN) activates the glucocorticoid receptor (GR) signaling pathway independent of the pregnane X receptor (PXR), and GR activation is required for the suppression of hippocampal cytochrome P450 enzyme expression and attenuation of phenytoin (PHT) neurotoxicity. (A–C) Wild-type (WT) male mice or PXR knockout (PXR KO) mice were treated with vehicle (VEH) or PCN for four weeks before analyses ($n = 6$). The messenger RNA (mRNA) expression of GR target genes in the liver (A, left) and hippocampus (A, right) were measured by real-time quantitative reverse transcription-polymerase chain reaction (RT-qPCR), and immunohistochemistry (IHC) staining of GR in the liver (B) and hippocampus (C) with the signaling semi-quantified by ImageJ scripts of IHC-Toolbox. (D–F) WT male mice were treated with VEH, PHT, PHT + PCN, or PHT + PCN + mifepristone (RU486) for four weeks before analyses ($n = 6$). The mRNA (D) and protein (E) expressions of cytochrome P450, family 3, subfamily a, polypeptide 11 (*CYP3A11*) and *CYP2B10* in the liver and hippocampus measured by RT-qPCR and Western blotting, respectively, and the hippocampal mRNA expression of *PSD95*, *SYN1*, *SYP*, and *SYT1* measured by RT-qPCR (F). Data are presented as mean ± standard error of the mean. $^*P < 0.05$ and $^{**}P < 0.01$. CON: control.
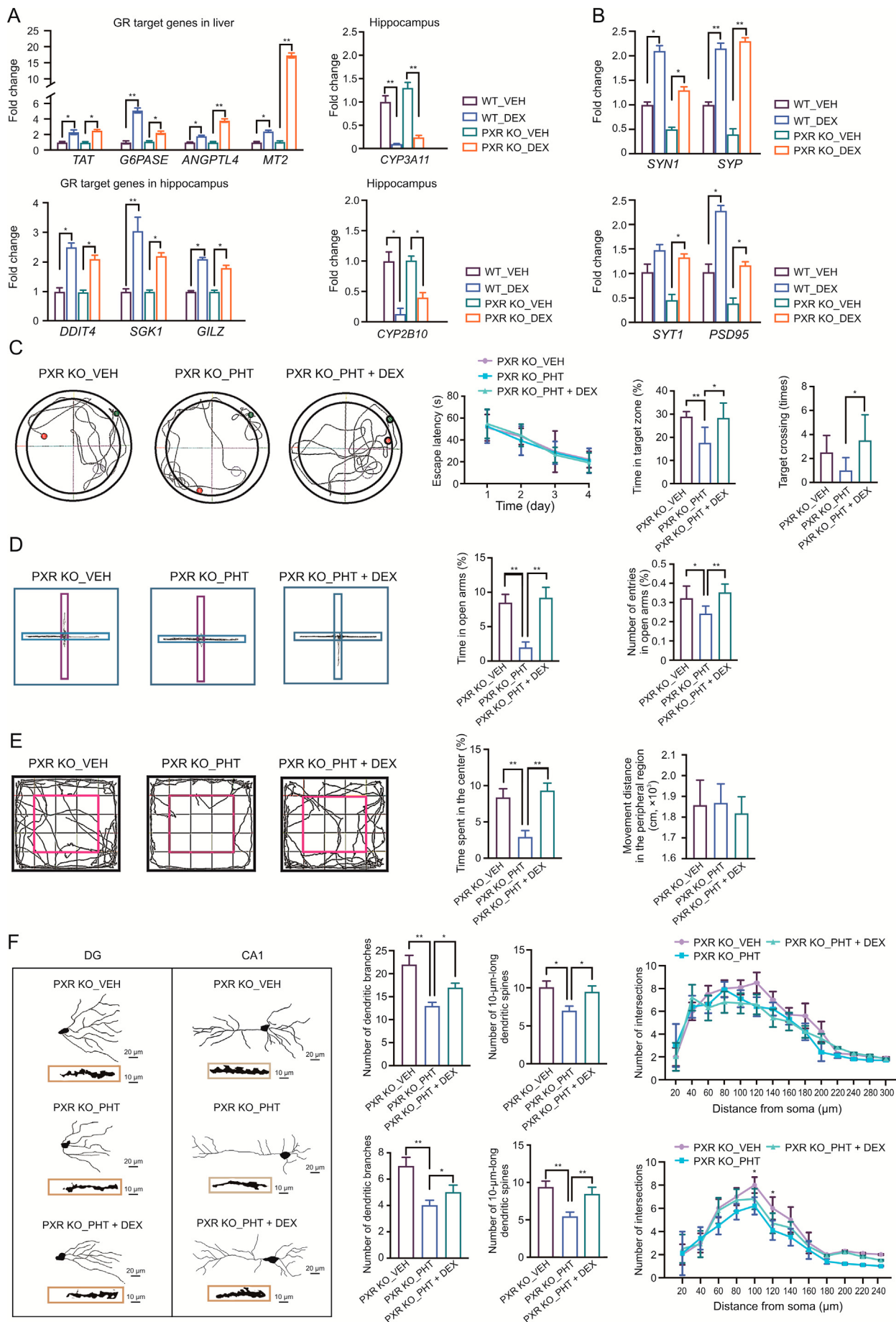
Subsequent Nissl staining of PXR KO mice revealed that PHT treatment decreased the number of Nissl positive neurons in the CA1 and DG regions, an effect that was effectively attenuated by co-treatment with PCN, as depicted in Fig. 4D. Additionally, optical density analysis of the entire stained hippocampus sections showed that PCN and PHT increased and decreased the staining intensity, respectively, and the staining intensity of the PHT + PCN group was significantly higher than that of the PHT group (Fig. 4D). Golgi staining revealed that PHT treatment alone reduced the number of hippocampal neuron branches and the density of dendritic spines of PXR KO mice in both the CA1 region (Fig. 4E, top middle two panels) and DG region (Fig. 4E, bottom middle two panels), an effect that was effectively attenuated by co-treatment with PCN. However, the number of intersections was not different in the CA1 region between the groups (Fig. 4E, top right panel), but the numbers of intersections in the DG region 100 and 120 μm away from the cell body were decreased in the PHT group compared to the control group (Fig. 4E, bottom right panel). Furthermore, PHT treatment inhibited the expression of *PSD95*, *SYN1*, *SYP*, and *SYT1* in PXR KO mice, as shown in Fig. 4F. Co-treatment with PCN attenuated the suppression of *PSD95* and *SYT1*, but the effect of PCN on the suppression of *SYN1* and *SYP* was not statistically significant. Notably, the general pattern of the PCN effect on PHT-induced neurobehavioral changes and hippocampal neurotoxicity in PXR KO mice was similar to that observed in WT mice, suggesting that the neuroprotective effect of PCN is independent of PXR.

3.5. Bioinformatic analysis reveals that PHT-induced neurotoxicity is accompanied by the suppression of GC/GR signaling in the hippocampus

To elucidate the mechanism underlying the neuroprotective effects of PCN against PHT-induced neurotoxicity, we analyzed the GEO dataset (GSE2880), a microarray dataset comparing gene expression between vehicle- and PHT-treated hippocampal tissues of rats. Our analysis revealed that the top 200 differentially expressed genes (DEGs) were indeed different between the vehicle and PHT groups, as depicted in the heat map presented in Fig. 5A. We subsequently selected DEGs (|logFC| > 0.5) for enrichment analysis of pathway and Gene Ontology (GO) term. Using the ClusterProfiler package, we performed Wiki pathway enrichment analysis of DEGs and observed that seven signaling pathways were enriched, including the 'Glucocorticoid metabolism' pathway, along with three pathways related to G-protein-coupled receptors (GPCRs) (Fig. 5B). Recent studies have suggested that glucocorticoids can work in concert with GPCRs to form complexes that play physiological roles [32]. These findings suggest that treatment with PHT affects glucocorticoid-related signaling pathways in the hippocampus. Our Kyoto Encyclopaedia of Genes and Genomes (KEGG) signaling pathway analysis revealed that the 'Steroid hormone biosynthesis' signaling was enriched, as illustrated in Fig. 5C. Additionally, our gene set enrichment analysis showed that the rank score for 'Steroid hormone biosynthesis' signaling in the PHT-treatment group was down-regulated, as depicted in Fig. 5D. To further confirm the results from the Wiki and KEGG analyses, we

conducted observation and verification in the GO term enrichment analysis. Our results, as presented in Fig. 5E, indicate that some hormone-related biological processes had changed significantly. For instance, the terms of 'Steroid metabolic process', 'Hormone metabolic process', 'Steroid catabolic process', and 'Glucocorticoid metabolic process' showed an upward trend. These pathway analysis results are consistent with reports indicating that PHT can accelerate the metabolism of glucocorticoids, thereby decreasing their biological activity [33–35]. These findings suggest that GC/GR related functional and signaling changes may play a crucial role in PHT-induced hippocampal injury. We then specifically examined the expression of GC/GR responsive genes in the microarray. The results depicted in Fig. 5F showed a down-regulation of the expressions of genes typically activated by GR, namely *Kat2b*, *Cav1*, *Per1*, *Trim63*, *Hdac1*, and *Ncoa1*, while the expressions of genes typically suppressed by GR, including *Jun*, *AP1*, *AR*, *Atp1b1*, and *Nr4a2*, were up-regulated in the PHT group, as illustrated in Fig. 5G. Furthermore, the study observed a down-regulation of the expression of GR (*Nr3c1*) itself in the PHT group, as presented in Fig. 5H. The results imply that the neurotoxicity of PHT could be attributed to the suppression of GC/GR signaling in the hippocampus. Although the study utilized rats, the high conservation of species of GR and its signaling motivated the researchers to concentrate on GR-related signaling modifications in their mechanistic investigations.

3.6. PCN regulates hippocampal CYP expression and attenuates PHT-induced neurotoxicity by activating the GC/GR signaling pathway

To investigate whether the neuroprotective effects of PCN are mediated by the activation of the GC/GR signaling pathway in the hippocampus, the study conducted an experiment using both WT and PXR KO mice. The mice were treated with PCN or vehicle, and the hepatic mRNA expression of GR target genes such as *ANGPTL4* and *MT2* was induced in both genotypes, as depicted in Fig. 6A (left panel). Additionally, the mRNA expression of GR target genes, including *DDIT4*, *FKBP5*, and *GILZ*, was also induced in the hippocampus of both genotypes, as shown in Fig. 6A (right panel). IHC staining revealed that PCN treatment induced the expression of GR in the liver of WT mice but not in PXR KO mice, as presented in Figs. 6B and S2M. In the hippocampus, PCN treatment induced the expression of GR in the CA1 and DG regions of both WT and PXR KO mice, as illustrated in Figs. 6C and S2N.

To investigate whether the neuroprotective effects of PCN in WT mice are mediated through the GC/GR signaling pathway, the study employed the GR antagonist RU486. The study observed that co-treatment with RU486 had minimal effects on the mRNA induction of *CYP3A11* and *CYP2B10* by the combined treatment of PHT and PCN in the liver (Fig. 6D). However, in the hippocampus, co-treatment with RU486 abolished the suppressive effect of PCN on PHT-responsive induction of *CYP3A11* and *CYP2B10* (Fig. 6D), indicating that GR activation was involved in the effect of PCN on the hippocampal expression of CYPs. The same pattern of RU486 effect was observed when the protein

Fig. 7. Pharmacological activation of the glucocorticoid receptor (GR) is sufficient to alleviate neurotoxicity caused by phenytoin (PHT) independent of the pregnane X receptor (PXR). (A, B) Wild-type (WT) male mice or PXR knockout (PXR KO) mice were treated with vehicle (VEH) or dexamethasone (DEX) for four weeks before analyses ($n = 8$). The messenger RNA (mRNA) expression of GR target genes in the liver and hippocampus (A, left), and hippocampal expression of cytochrome P450, family 3, subfamily a, polypeptide 11 (*CYP3A11*) and *CYP2B10* (A, right), and hippocampal mRNA expression of *PSD95*, *SYN1*, *SYP*, and *SYT1* (B) measured by real-time quantitative reverse transcription-polymerase chain reaction (RT-qPCR). (C–F) Male PXR KO mice were treated with vehicle, PHT, or PHT + DEX for four weeks before analyses ($n = 6$). Morris water maze results with the escape latency recorded, and the crossing number and residence time in the target quadrant calculated (C), elevated plus maze results with the elevated activity track, the stay time, and the entry number in the open arms calculated (D), open field test results with the residence time in the central area and the movement distance in the peripheral region calculated (E), and Golgi staining of the hippocampus sections with the representative images of the neurite tracing profiles of neurons in the cornu ammonis area 1 (CA1) and dentate gyrus (DG) region (F). Data are presented as mean ± standard error of the mean. $^{*}P < 0.05$ and $^{**}P < 0.01$.

level of CYP3A11 and CYP2B10 in the liver (Fig. 6E, top panels) and hippocampus (Fig. 6E, bottom panels) was evaluated by Western blotting. Upon evaluating the mRNA expression of hippocampal synaptic genes, the study observed that the suppressive effect of PHT on *PSD95*, *SYN1*, and *SYP* was attenuated by PCN in WT mice. However, co-treatment with RU486 diminished the neuroprotective effects of PCN on the expression of *PSD95*, *SYN1*, and *SYP* (Fig. 6F).

To investigate whether pharmacological activation of GR is sufficient to alleviate PHT-induced neurobehavioral changes and hippocampal neurotoxicity, and whether these effects are PXR-dependent, the study treated both WT and PXR KO mice with DEX (GR agonist). The dose of DEX administered was 4 mg/kg/day, which was expected to activate GR but not PXR [36]. The study observed an induction of hepatic and hippocampal expressions of GR target genes in both genotypes upon DEX administration, as illustrated in Fig. 7A (left panels), verifying that the GR activation effect of DEX was independent of PXR. The effects of DEX on hippocampal CYP expression were comparable to those of PCN, suppressing the expression of *CYP3A11* and *CYP2B10* in the hippocampus in both genotypes, as shown in Fig. 7A (right panels). Moreover, the mRNA expression of synaptic genes *PSD95*, *SYN1*, *SYP*, and *SYT1* was induced by DEX in both WT and PXR KO mice, as presented in Fig. 7B, similar to the pattern observed with PCN. To further confirm that the effect of DEX in PXR KO was mediated by GR, the study evaluated the combined effect of DEX and RU486. The results showed that DEX reversed PHT-induced hippocampal expression of *CYP3A11* and *CYP2B10*, but this effect was abolished in mice co-treated with RU486, as depicted in Fig. S5A. Additionally, DEX partially reversed PHT-responsive suppression of synaptic protein expression, and this effect was also abolished by RU486, as shown in Fig. S5B.

We evaluated the effect of DEX on PHT-induced neurobehavioral changes and hippocampal neurotoxicity in PXR KO mice. The Morris water maze test showed that PHT treatment reduced the residence time of PXR KO mice in the target quadrant, which was reversed by DEX co-treatment, as depicted in Fig. 7C. In the elevated plus maze test, PHT treatment decreased open arm stay time and open arm entry times, which was also reversed by DEX co-treatment, as presented in Fig. 7D. Additionally, in the open field test, PHT treatment decreased the time taken in the central area without affecting total distance travelled, which was reversed by DEX co-treatment, as shown in Fig. 7E. The study also evaluated the Golgi staining on the hippocampus tissue sections of PXR KO mice. In the CA1 region, PHT reduced the number of dendritic branches and density of dendritic spines without affecting the number of intersections, and this effect was attenuated by the co-treatment of DEX, as illustrated in Fig. 7F (top panels). In the DG region, PHT reduced the density of dendritic spines and the number of dendritic branches and intersections, and this effect was also attenuated by DEX co-treatment, as presented in Fig. 7F (bottom panels). These results suggest that the GR-activating dose of DEX attenuates PHT-induced neurotoxicity independently of PXR.

4. Discussion

There were several unexpected findings in this study. The first surprise is the differential effect of PCN on the expression of CYPs in the liver and hippocampus. PCN is best known for its agonistic activity towards PXR. PCN has been reported to induce the hepatic expression of CYPs in a PXR dependent manner [16], which was further confirmed in the current study. To our surprise, the hippocampal expression of CYP3A11 and CYP2B10 was found to be suppressed in the same PCN-treated mice. To our knowledge, this is

the first report that PCN had a tissue-dependent effect on the expression of CYPs.

The second surprise was the mechanism by which PCN suppresses the expression of hippocampal CYPs. Although PCN is best known for activating PXR and inducing the hepatic expression of CYPs, we found the suppression of hippocampal CYPs by PCN was independent of PXR, because PCN remained effective in suppressing hippocampal CYPs in PXR KO mice. Instead, and through gene expression profiling and use of the established GR antagonist RU486, the suppression of hippocampal CYPs by PCN was found to be associated with the activation of GR, and the hippocampal CYP suppressive effect of PCN was abolished in mice co-treated with RU486. We further showed that treatment of mice with the GR agonist DEX was sufficient to suppress the expression of hippocampal CYPs. These results suggest that co-administration of glucocorticoids might be a strategy to manage the neuronal side effects of PHT. Indeed, glucocorticoids have been used to treat epilepsy syndrome and drug-resistant epilepsy as an additional treatment [37,38].

CYPs, such as CYP3As, CYP2Bs, and CYP2Cs, are better known for their expression, regulation, and function in the liver and intestines [1,39]. Our results have provided convincing evidence that these CYPs are also expressed and transcriptionally regulated in the central nervous system. Moreover, the expression and regulation of hippocampal CYPs have their implications in the metabolism of endobiotics such as androgens, as well as conceivably xenobiotics such as drugs and environmental chemicals.

Our results are clinically relevant. The use of PHT is known to have potential side effects of anxiety and cognitive impairment [40–43], which were recapitulated in our mice treated with PHT. Mechanistically, our results strongly suggested that PHT-induced neurobehavioral changes and hippocampal neurotoxicity were likely caused by PHT-responsive induction of hippocampal CYPs and the consequent increase in the metabolic deactivation of TES, a neuroactive steroid important for neurophysiological functions, such as emotion, cognition, and behavior [44]. Our speculation that depletion of TES contributes to the neuronal side effects of PHT is consistent with the notion that decreased central levels of TES play a role in the neuronal side effects of PHT [29]. The serum levels of bioavailable TES, including free TES and albumin-bound TES, were significantly reduced in male temporal lobe epilepsy patients, which were accompanied by clinical manifestations, including low libido, impotence, depression, and cognitive decline [45,46]. Interestingly, these behavioral changes were more pronounced in patients treated with P450-inducing drugs, such as PHT, than in patients treated with non-inducer drugs [6,28]. It has been reported that changes in the total TES level of epilepsy patients mainly occur in the hippocampus rather than the serum [47], suggesting that the hippocampal CYPs are particularly important in TES metabolism and may be involved in the neurotoxic side effects of antiepileptic drugs.

There are several limitations in this study. 1) As shown in Figs. 3 and 4, in WT mice, PCN could reverse the expression of synaptic genes in PHT-treated mice to the level of the vehicle control group, and the corresponding neurobehaviors such as anxiety, depression, learning, and memory impairment were also improved. However, when nerve damage was evaluated by Golgi staining, the reversal effect of PCN was mainly in the hippocampal CA1 region, but not in the DG region, which may be due to the fact that PHT was not effective in inducing DG pathology in our model . However, in PXR KO mice, PCN ameliorated PHT-induced hippocampal nerve damage in CA1 and DG regions. It is possible that PHT caused more severe nerve damage in PXR KO mice including the DG region, so PCN showed a better improvement effect. 2) Our results suggest that PCN activated hippocampal GR. As for the effect of PCN on liver

GR, the early literature suggested that PCN can antagonize liver GR [48], but whether this is the reason for the differential effect of PCN on CYP expression in the hippocampus and liver needs further studies, including the creation and use of liver and hippocampus specific GR KO mice. 3) Although we found that PCN could attenuate the neurotoxic side effects of PHT, but the neuroprotective effect of PCN has not yet been verified in an epilepsy model. 4) We cannot exclude the potential involvement of another xenobiotic receptor, CAR. PHT has been reported to regulate CYPs by activating CAR [13]. The future use of CAR knockout mice is necessary to exclude the role of CAR in mediating the neurotoxicity of PHT and attenuation of this side effect by PCN. 5) Another limitation of this study is the possible species differences in nuclear receptor activation and response. Moreover, the translation of our animal data to the human situation warrants future studies.

5. Conclusion

In summary, the study reports that PCN, a prototypical PXR agonist, suppressed the expression of CYPs in the hippocampus in a tissue-specific manner. PCN displayed neuroprotective effects by inhibiting the expression of hippocampal CYPs and preserving TES activity through the activation of the GC/GR signaling pathway, thereby attenuating PHT-induced hippocampal nerve injury. Although PCN is not a clinical drug, the study suggests that glucocorticoids could be used to alleviate the neuronal side effects of PHT.

CRediT author statement

Shuai Zhang: Visualization, Software, Formal analysis, Data curation, Methodology, Writing - Original draft preparation, Validation; **Tingting Wang:** Writing - Reviewing and Editing; **Ye Feng:** Formal analysis; **Fei Li** and **Aijuan Qu:** Resources; **Xiuchen Guan:** Software; **Hui Wang:** Conceptualization, Project administration, Funding acquisition; **Dan Xu:** Conceptualization, Formal analysis, Resources, Validation, Methodology, Investigation, Writing - Reviewing and Editing, Funding acquisition.

Declaration of competing interest

The authors declare that there are no conflicts of interest.

Acknowledgments

Appendix A. Supplementary data

Supplementary data to this article can be found online at https://doi.org/10.1016/j.jpha.2023.07.013.

References

[1] P. Anzenbacher, E. Anzenbacherová, Cytochromes P450 and metabolism of xenobiotics, Cell, Mol. Life Sci. 58 (2001) 737−747.
[2] W. Kuban, W.A. Daniel, Cytochrome P450 expression and regulation in the brain, Drug Metab. Rev. 53 (2021) 1−29.
[3] B. Schilter, C.J. Omiecinski, Regional distribution and expression modulation of cytochrome P-450 and epoxide hydrolase mRNAs in the rat brain, Mol. Pharmacol. 44 (1993) 990−996.
[4] S.L. Miksys, R.F. Tyndale, Drug-metabolizing cytochrome P450s in the brain, J. Psychiatry Neurosci. 27 (2002) 406−415.
[5] A.G. Herzo, L.A. Levesque, F.W. Drislane, et al., Phenytoin-induced elevation of serum estradiol and reproductive dysfunction in men with epilepsy, Epilepsia 32 (1991) 550−553.
[6] J.I.T. Isojärvi, E. Taubøll, A.G. Herzog, Effect of antiepileptic drugs on reproductive endocrine function in individuals with epilepsy, CNS Drugs 19 (2005) 207−223.
[7] A. Quartier, L. Chatrousse, C. Redin, et al., Genes and pathways regulated by androgens in human neural cells, potential candidates for the male excess in autism spectrum disorder, Biol. Psychiatry 84 (2018) 239−252.
[8] M.I. Ransome, W.C. Boon, Testosterone-induced adult neurosphere growth is mediated by sexually-dimorphic aromatase expression, Front. Cell. Neurosci. 9 (2015), 253.
[9] M.D. Spritzer, L.A.M. Galea, Testosterone and dihydrotestosterone, but not estradiol, enhance survival of new hippocampal neurons in adult male rats, Dev. Neurobiol. 67 (2007) 1321−1333.
[10] T.S. Benice, J. Raber, Castration and training in a spatial task alter the number of immature neurons in the hippocampus of male mice, Brain Res 1329 (2010) 21−29.
[11] G. Corona, F. Guaraldi, G. Rastrelli, et al., Testosterone deficiency and risk of cognitive disorders in aging males, World J. Mens Health 39 (2021) 9−18.
[12] F. Kurth, E. Luders, N.L. Sicotte, et al., Neuroprotective effects of testosterone treatment in men with multiple sclerosis, Neuroimage Clin 4 (2014) 454−460.
[13] H. Wang, S. Faucette, R. Moore, et al., Human constitutive androstane receptor mediates induction of *CYP2B6* gene expression by phenytoin, J. Biol. Chem. 279 (2004) 29295−29301.
[14] J.P. Jackson, S.S. Ferguson, R. Moore, et al., The constitutive active/androstane receptor regulates phenytoin induction of Cyp2c29, Mol. Pharmacol. 65 (2004) 1397−1404.
[15] P. Torres-Vergara, Y.S. Ho, F. Espinoza, et al., The constitutive androstane receptor and pregnane X receptor in the brain, Br. J. Pharmacol. 177 (2020) 2666−2682.
[16] W. Xie, J.L. Barwick, M. Downes, et al., Humanized xenobiotic response in mice expressing nuclear receptor SXR, Nature 406 (2000) 435−439.
[17] C.D. Applegate, G.M. Samoriski, K. Özduman, Effects of valproate, phenytoin, and MK-801 in a novel model of epileptogenesis, Epilepsia 38 (1997) 631−636.
[18] S. Sudha, M.K. Lakshmana, N. Pradhan, Chronic phenytoin induced impairment of learning and memory with associated changes in brain acetylcholine esterase activity and monoamine levels, Pharmacol. Biochem. Behav. 52 (1995) 119−124.
[19] A. Mohan, K. Krishna, Memory impairment allied to temporal lobe epilepsy and its deterioration by phenytoin: A highlight on ameliorative effects of levetiracetam in mouse model, Int. J. Epilepsy 5 (2018) 19−27.
[20] V. Zoufal, S. Mairinger, M. Brackhan, et al., Imaging P-glycoprotein induction at the blood-brain barrier of a β-amyloidosis mouse model with ^{11}C-metoclopramide PET, J. Nucl. Med. 61 (2020) 1050−1057.
[21] B. Bauer, A.M. Hartz, G. Fricker, et al., Pregnane X receptor up-regulation of P-glycoprotein expression and transport function at the blood-brain barrier, Mol. Pharmacol. 66 (2004) 413−419.
[22] T. Yılmaz, M. Akça, Y. Turan, et al., Efficacy of dexamethasone on penicillin-induced epileptiform activity in rats: An electrophysiological study, Brain Res. 1554 (2014) 67−72.
[23] Y. Zhang, W. Hu, B. Zhang, et al., Ginsenoside Rg1 protects against neuronal degeneration induced by chronic dexamethasone treatment by inhibiting NLRP-1 inflammasomes in mice, Int. J. Mol. Med. 40 (2017) 1134−1142.
[24] B.W. Peeters, J.A. Tonnaer, M.B. Groen, et al., Glucocorticoid receptor antagonists: New tools to investigate disorders characterized by cortisol hypersecretion, Stress 7 (2004) 233−241.
[25] J. Shu, G. Qiu, I. Mohammad, semi-automatic image analysis tool for biomarker detection in immunohistochemistry analysis, 2013 Seventh International Conference on Image and Graphics. July 26−28, 2013, Qingdao, China. IEEE, 2013, pp. 937−942.
[26] A.T.M. Konkle, M.M. McCarthy, Developmental time course of estradiol, testosterone, and dihydrotestosterone levels in discrete regions of male and female rat brain, Endocrinology 152 (2011) 223−235.
[27] B.N. DuBois, F. Amirrad, R. Mehvar, A comparison of calcium aggregation and ultracentrifugation methods for the preparation of rat brain microsomes for drug metabolism studies, Pharmacology 106 (2021) 687−692.
[28] P.M. Jeavons, Letter: Behavioural effects of anti-epileptic drugs, Dev. Med. Child Neurol. 18 (1976), 394.
[29] R.P. Meyer, C.E. Hagemeyer, R. Knoth, et al., Anti-epileptic drug phenytoin enhances androgen metabolism and androgen receptor expression in murine hippocampus, J. Neurochem. 96 (2006) 460−472.
[30] C. Ghosh, M. Hossain, A. Spriggs, et al., Sertraline-induced potentiation of the CYP3A4-dependent neurotoxicity of carbamazepine: An *in vitro* study, Epilepsia 56 (2015) 439−449.
[31] T. Niwa, N. Murayama, Y. Imagawa, et al., Regioselective hydroxylation of steroid hormones by human cytochromes P450, Drug Metab. Rev. 47 (2015) 89−110.
[32] Y.-Q. Ping, C. Mao, P. Xiao, et al., Structures of the glucocorticoid-bound adhesion receptor GPR97-G$_o$ complex, Nature 589 (2021) 620−626.
[33] C. Kara, A. Ucaktürk, O.F. Aydin, et al., Adverse effect of phenytoin on glucocorticoid replacement in a child with adrenal insufficiency, J. Pediatr. Endocrinol. Metab. 23 (2010) 963−966.

[34] J.B. Chalk, K. Ridgeway, T. Brophy, et al., Phenytoin impairs the bioavailability of dexamethasone in neurological and neurosurgical patients, J. Neurol. Neurosurg. Psychiatry 47 (1984) 1087–1090.

[35] W. Jubiz, A.W. Meikle, Alterations of glucocorticoid actions by other drugs and disease states, Drugs 18 (1979) 113–121.

[36] S.R. Hunter, A. Vonk, A.K. Mullen Grey, et al., Role of glucocorticoid receptor and pregnane X receptor in dexamethasone induction of rat hepatic aryl hydrocarbon receptor nuclear translocator and NADPH-cytochrome P450 oxidoreductase, Drug. Metab. Dispos. 45 (2017) 118–129.

[37] E. Haberlandt, C. Weger, S.B. Sigl, et al., Adrenocorticotropic hormone versus pulsatile dexamethasone in the treatment of infantile epilepsy syndromes, Pediatr. Neurol. 42 (2010) 21–27.

[38] S. Shorvon, M. Ferlisi, The treatment of super-refractory status epilepticus: A critical review of available therapies and a clinical treatment protocol, Brain 134 (2011) 2802–2818.

[39] K. Thelen, J.B. Dressman, Cytochrome P450-mediated metabolism in the human gut wall, J. Pharm. Pharmacol. 61 (2009) 541–558.

[40] A.M. Kanner, M.M. Bicchi, Antiseizure medications for adults with epilepsy: A review, JAMA 327 (2022) 1269–1281.

[41] J. Patocka, Q. Wu, E. Nepovimova, et al., Phenytoin–An anti-seizure drug: overview of its chemistry, pharmacology and toxicology, Food. Chem. Toxicol. 142 (2020), 111393.

[42] J.D. Cardoso-Vera, L.M. Gómez-Oliván, H. Islas-Flores, et al., Multi-biomarker approach to evaluate the neurotoxic effects of environmentally relevant concentrations of phenytoin on adult zebrafish *Danio rerio*, Sci. Total Environ. 834 (2022), 155359.

[43] M.M. Nagib, M.G. Tadros, R.M. Rahmo, et al., Ameliorative effects of α-tocopherol and/or coenzyme Q10 on phenytoin-induced cognitive impairment in rats: Role of VEGF and BDNF-TrkB-CREB pathway, Neurotox. Res. 35 (2019) 451–462.

[44] B.S. McEwen, How do sex and stress hormones affect nerve cells? Ann. N. Y. Acad. Sci. 743 (1994) 1–18.

[45] A.G. Herzog, K.M. Fowler, Sexual hormones and epilepsy: Threat and opportunities, Curr. Opin. Neurol. 18 (2005) 167–172.

[46] C.A. Frye, Role of androgens in epilepsy, Expert Rev. Neurother. 6 (2006) 1061–1075.

[47] N. Killer, M. Hock, M. Gehlhaus, et al., Modulation of androgen and estrogen receptor expression by antiepileptic drugs and steroids in hippocampus of patients with temporal lobe epilepsy, Epilepsia 50 (2009) 1875–1890.

[48] E.G. Schuetz, W. Schmid, G. Schutz, et al., The glucocorticoid receptor is essential for induction of cytochrome P-4502B by steroids but not for drug or steroid induction of CYP3A or P-450 reductase in mouse liver, Drug Metab. Dispos. 28 (2000) 268–278.